Enhancement of upconversion luminescence of Er doped Al2O3 films by Ag island films

Aisaka, Takeho
Fujii, Minoru
Hayashi, Shinji

(Citation)
Applied Physics Letters,92(13):132105-132105

(Issue Date)
2008-04

(Resource Type)
journal article

(Version)
Version of Record

(URL)
https://hdl.handle.net/20.500.14094/90000678

Enhancement of upconversion luminescence of Er doped Al_2O_3 films by Ag island films

Takeho Aisaka, Minoru Fujii,[a] and Shinji Hayashi
Department of Electrical and Electronics Engineering, Faculty of Engineering, Kobe University, Rokkodai, Nada, Kobe 657-8501, Japan

(Received 5 October 2007; accepted 20 February 2008; published online 1 April 2008)

Strong enhancement of upconversion photoluminescence (PL) of Er^{3+} in the visible range was achieved by placing it near rough Ag island films. In order to understand the mechanism of the enhancement, PL was excited by 978 and 488 nm light and the enhancement factors were obtained in a wide spectral range (520 nm to 1.6 μm). The emission and excitation wavelength dependence of the enhancement factors revealed that both the incident electric fields and the radiative decay rate of Er^{3+} are enhanced due to the excitation of surface plasmons supported by Ag islands. It was found that the upconversion PL is more sensitive to the enhancement of the incident electric field than the downconversion PL because of the multiphoton absorption process. The present result indicates that the upconversion PL obtains more benefit from the metal-enhanced fluorescence technique than the downconversion PL. © *2008 American Institute of Physics*. [DOI: 10.1063/1.2896303]

In recent years, upconversion luminescence of rare-earth doped materials has attracted much interest in their capability of converting infrared radiation into visible light. One of the well studied systems is Er-doped glasses, which show green and red photoluminescence (PL) under excitation by near-infrared (NIR) light. Since low-cost and high-power NIR laser diodes are available for the excitation source, Er-doped glasses are of great interest for applications such as lasers,[1] three-dimensional displays,[2] and biological fluorescence imaging.[3–6] However, the photon absorption cross section of Er^{3+} is very small due to the dipole-forbidden nature of the intra-4*f* transitions and, thus, the intensity of the upconversion PL is relatively low. In order to overcome the small absorption cross section, Yb^{3+} is usually doped simultaneously as a photosensitizer.

In this work, we will show another approach to enhance the upconversion luminescence of Er^{3+}. It has been demonstrated for different kinds of materials that the luminescence intensity of emitters is strongly enhanced when they are placed near metal nanostructures (metal-enhanced fluorescence).[7–11] The enhancement is caused by the excitation of surface plasmons (SPs) supported by metal nanostructures. The enhancement mechanism can be classified into two categories, i.e., the enhancement of an electric field of incident light and the enhancement of the radiative decay rate. In this work, we apply the same strategy to the upconversion PL of Er^{3+}. A similar approach was reported for Er-doped heavy-metal oxide glasses containing silver nanoparticles. However, the degree of the enhancement was not very large and the role of SP excitation on the PL enhancement was not clarified.[12]

One of the purposes of this work is to achieve a large enhancement of upconversion PL of Er^{3+} by placing it on Ag island films with different morphologies. Another purpose is to clarify the mechanism of the PL enhancement. To achieve this, we measure upconversion and downconverson PL excited at 978 nm and downconversion PL excited at 488 nm, and obtain PL enhancement factors in a wide wavelength range. By comparing the wavelength dependence of the enhancement factors with that of SP absorption spectra of Ag islands and by comparing the enhancement factors of upconversion and downconversion PL, the relative contributions of two enhancement processes are discussed.

Samples studied are Er doped Al_2O_3 films about 130 nm in thickness deposited on fused quartz substrates. Al_2O_3 and Er_2O_3 sputtering targets were simultaneously sputtered in Ar gas of 2.7 Pa using a rf magnetron sputtering apparatus. The films were then annealed in N_2 gas atmosphere at 900 °C for 30 min. The Er concentration was fixed to about 4.2 at. %. In this Er concentration range, cooperative upconversion plays a major role for the visible PL.[13] After the annealing, Ag thin films approximately 7, 10, 13, and 16 nm in thicknesses were deposited by vacuum evaporation. The deposition rate monitored by a quartz crystal microbalance was 0.02 nm/s. After the deposition, the samples were annealed at 300 °C for 1 h.

Figure 1 shows atomic force microscope (AFM) (Seiko Instruments Inc. NPX200) images of sample surface. The thicknesses of Ag films are changed from 7 to 16 nm. We can see that the size of Ag particles and the distance between

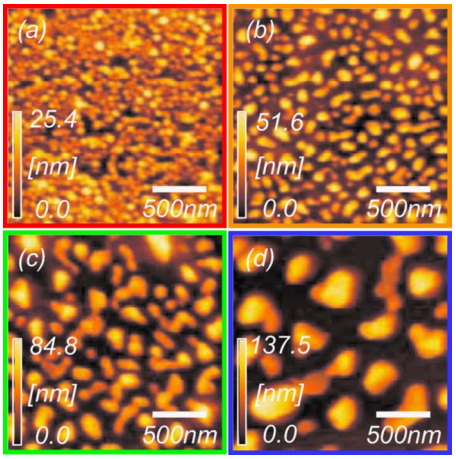

FIG. 1. (Color online) AFM images of Ag island films deposited on Er-doped Al_2O_3 thin films. The mass thicknesses are (a) 7, (b) 10, (c) 13, and (d) 16 nm. The average diameters are (a) 104, (b) 147, (c) 219, and (d) 313 nm and the average heights are (a) 16, (b) 28, (c) 52, and (d) 91 nm.

[a]Author to whom correspondence should be addressed. Electronic mail: fujii@eedept.kobe-u.ac.jp.

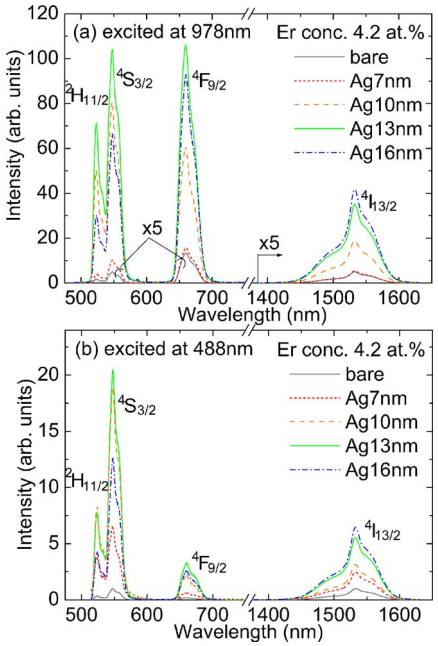

FIG. 2. (Color online) PL spectra of Er-doped Al_2O_3 thin films with and without Ag island films on top excited at (a) 978 and (b) 488 nm. The mass thicknesses of Ag island films are 7, 10, 13, and 16 nm. Four main peaks correspond to transitions from $^2H_{11/2}$, $^4S_{3/2}$, $^4F_{9/2}$, and $^4I_{13/2}$ states to $^4I_{15/2}$ state of Er^{3+}. Spectra below and above 800 nm are normalized by the intensity of $^4S_{3/2}$ and $^4I_{13/2}$ peaks, respectively, of the sample without a Ag island film. In (a), spectra below 800 nm for the samples without a Ag island film and with 7-nm-thick Ag film and spectra above 800 nm for all the samples are multiplied by 5.

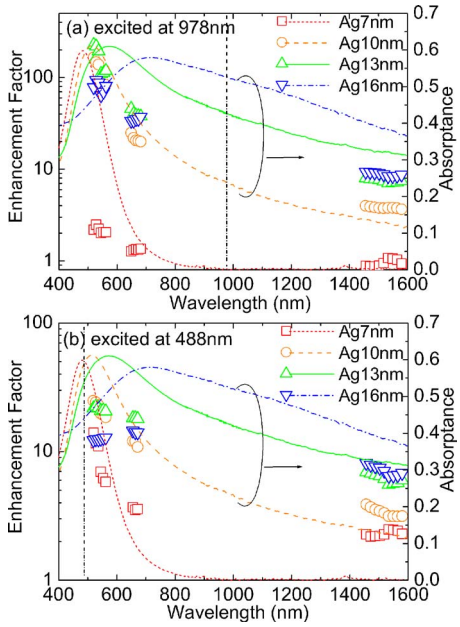

FIG. 3. (Color online) Enhancement factors obtained by dividing PL spectra of samples with Ag islands by those without Ag islands (symbols) (left axis). Excitation wavelengthes are (a) 978 and (b) 488 nm. For comparison, absorptance (1-transmittance-reflectance) spectra are also shown (right axis). Note that the same absorptance spectra are shown in (a) and (b).

them increase as the mass thickness increases. The average diameters are (a) 104, (b) 147, (c) 219, and (d) 313 nm and the average heights are (a) 16, (b) 28, (c) 52, and (d) 91 nm. For these samples, optical transmittance (T) and reflectance (R) were measured in the 400–1600 nm range using a UV-visible-NIR scanning spectrometer (Shimadzu UV-3101) and the absorptance, which is defined as 1-T-R, was obtained.

For the PL measurements, samples were excited by 978 nm light from a cw Ti:sapphire laser or a 488 nm line of an Ar ion laser. PL excitation was made from the substrate side about 45° from the normal to the surface and PL to the normal to the surface was collected from the same side. PL spectra were recorded using a single grating monochromator equipped with a charge coupled device for visible PL or with an InGaAs diode array for NIR PL. All the measurements were performed at room temperature.

Figures 2(a) and 2(b) show PL spectra excited at 978 and 488 nm, respectively. Three peaks in the visible range are assigned to the transitions from the $^2H_{11/2}$, $^4S_{3/2}$, and $^4F_{9/2}$ states to the ground state ($^4I_{15/2}$), respectively, and a peak in the NIR range to the $^4I_{13/2}$ to $^4I_{15/2}$ transition. The three peaks in the visible range in Fig. 2(a) are upconversion PL and the other peaks are downconversion PL. The spectra below 800 nm are normalized to the intensity of the $^4S_{3/2}$ peak of the sample without Ag islands and those above 800 nm to that of the $^4I_{13/2}$ peak. Figure 2(a) clearly demonstrates that PL intensities are strongly enhanced when Ag island films exist and the degree of the enhancements depends on the thickness of the films. Furthermore, the enhancement is much larger for the upconversion PL in the visible range than for the downconversion PL in the NIR range.

Similar enhancement of PL intensities are observed when the samples are excited at 488 nm [Fig. 2(b)]. However, the enhancement in the visible range is much smaller than that in Fig. 2(a). At this excitation wavelength, broad background PL, apparently differing from Er^{3+} PL, appears. The broad PL is considered to arise from oxides on the surface of Ag islands or emission of SPs supported by Ag islands. In order to extract the information of Er^{3+} PL, we subtracted PL spectra of Ag island films deposited on fuzed quartz substrates from those of the samples. The spectra shown in Fig. 2(b) are those after the subtraction.

To discuss the degree of PL enhancement in more detail, wavelength dependence of enhancement factors are obtained by dividing PL spectra of the samples with Ag islands by those without Ag islands. The divided spectra for 978 and 488 nm excitation are shown in Figs. 3(a) and 3(b), respectively, by symbols (left axis). Note that the data of the divided spectra are limited in specific wavelength ranges because of discrete PL bands of Er^{3+}. The absorptance spectra are also shown in the same figure (right axis) to discuss the PL enhancement mechanism. Broad absorption bands due to SP resonance of Ag islands can be seen. The SP resonance shifts to longer wavelengths and broadens as the Ag island films become thick, i.e., the Ag particles become large, due mainly to the retardation effect.[14,15]

In Fig. 3(a), we can see that the upconversion PL is strongly enhanced at around 520 nm, except for the sample with the thinnest Ag film. The maximum enhancement factor reaches 220 for the sample with a 13-nm-thick Ag film. Compared to this, the enhancement factors of downconversion PL at 1.54 μm are very limited (at maximum 9). This large difference of the enhancement factors between visible and NIR PL cannot be seen when the spectra are excited at 488 nm [Fig. 3(b)]. In this case, the maximum enhancement factor in the visible range is 25, while that in the NIR range is 8.

In general, metal-enhanced fluorescence arises from the enhancement of an electric field of incident light and also from that of the radiative decay rate. The distinction of these

two contributions is usually not simple but rough estimation of relative contributions is possible from the data in Fig. 3. We start from the simplest case in Fig. 3(b), where the excitation is made to the $^4F_{7/2}$ state by one photon absorption. In this case, the degree of the incident field enhancement is independent of the emission wavelength. Therefore, the observed wavelength dependence of the enhancement factors reflects that of the radiative decay rate. In the first approximation, the radiative decay rate is strongly enhanced at the wavelength where SPs are efficiently excited, i.e., the wavelength where the absorptance is large. In fact, we can see in Fig. 3(b) that wavelength dependence of the enhancement factors is quite similar to that of the absorptance of Ag islands.

In Fig. 3(b), for the sample with a 7-nm-thick Ag film, the absorptance in the NIR region (around 1.54 μm) is 0. This means that the small PL enhancement in this region (factor of about 2.5) is purely due to the enhancement of incident electric field. The maximum enhancement factor for the sample is about 14 at 520 nm. Therefore, in this sample, the PL enhancement due to the enhancement of electric fields of incident light is about 2.5 and that due to the radiative decay rate enhancement is about 5.6 at 520 nm, resulting in the total enhancement factor of 14.

Similar discussion can be made for the same sample excited at 978 nm [Fig. 3(a)]. In this case, the absorptance at the excitation wavelength is also 0 and, thus, no enhancement of NIR PL is expected. In fact, the enhancement factors of the sample around 1.54 μm are almost unity. In contrast, upconversion PL of the same sample in the visible range is slightly enhanced and the enhancement factor depends on the wavelength. Since the incident electric field is not enhanced, the observed PL enhancement is purely due to the enhancement of the radiative decay rate. We see that the radiative decay rate enhancement at 520 nm is about 2.5. This value is about a half of that obtained above for 488 nm excitation. The reason for the disagreement is not clear but it probably arises from the fact that the subtraction of the background signal caused by Ag islands at 488 nm excitation is not perfect.

In Fig. 3(a), the enhancement factors in the visible range for the samples with Ag films thicker than 10 nm are much larger than that for the sample with a 7-nm-thick Ag film. The significant difference in the enhancement factors can be attributed to whether the incident electric field is enhanced or not. Samples except for that with a 7-nm-thick Ag film have strong absorption at 978 nm due to the excitation of SPs in Ag islands. This result strongly suggests that in upconversion PL, the enhancement of incident electric fields play a significant role in the strong PL enhancement.

For cooperative upconversion of Er^{3+}, multiphotons are required to obtain one visible photon and the emission intensity (I_{up}) is proportional to the nth power of the excitation intensity (I_{exc}), $I_{up} \propto I_{exc}^n$, where n is the number of excitation photons required for emission of one visible photon.[16–18] Therefore, the upconversion PL intensity is proportional to the $2n$th power of the incident field intensity in contrast to the square of that in the case of downconversion PL. This means that upconversion PL can obtain more benefit from the strong electric fields of SPs than downconversion PL. This results in significant differences of the enhancement factors between the visible upconversion PL and the NIR downconversion PL in Fig. 3(a) or between the visible upconversion PL in Fig. 3(a) and the visible downconversion PL in Fig. 3(b).

As discussed above, in the first approximation, the wavelength dependence of the enhancement factors reflects that of the radiative decay rate enhancement. However, this model is not applicable to upconversion PL if the excitation processes are different at different emission bands. The number of photons (n) required for upconversion PL can be obtained from the slope of a $\log I_{up}$ versus $\log I_{exc}$ plot. For the present samples, n for 520 and 660 nm PL were 2.0 and 1.7, respectively. This indicates that the 520 nm PL enjoys the benefit of the incident field enhancement more than the 660 nm PL. This results in large difference of the enhancement factors of the upconversion PL between 520 and 660 nm. In fact, the differences in the enhancement factors between 520 and 660 nm are larger for the upconversion PL [Fig. 3(a)] than the downconversion PL [Fig. 3(b)] for almost all the samples.

In conclusion, we have succeeded in achieving strong enhancement of upconversion PL of Er^{3+} by placing it near Ag island films. The maximum enhancement factors of 220 was achieved for the 520 nm emission. The present results indicate that both the incident electric fields and the radiative decay rates are enhanced and the combination of them results in strong upconversion PL. We also demonstrated that in upconversion PL because of the multiphoton absorption process, the intensity is much more sensitive to the field intensity of incident light than that of downconversion PL. Therefore, by tuning the maximum of the SP absorption at 978 nm, much stronger upconversion PL is expected.

This work is supported by a Grant-in-Aid for Scientific Research from the Ministry of Education, Culture, Sports, Science and Technology, Japan.

[1] E. Heumann, S. Bär, K. Rademaker, G. Huber, S. Butterworth, A. Diening, and W. Seelert, Appl. Phys. Lett. **88**, 061108 (2006).
[2] E. Downing, L. Hesselink, J. Ralston, and R. Macfarlane, Science **273**, 1185 (1996).
[3] H. J. M. A. A. Zijlmans, J. Bonnet, J. Burton, K. Kardos, T. Vail, R. S. Niedbala, and H. J. Tanke, Anal. Biochem. **267**, 30 (1999).
[4] F. van de Rijke, H. Zijlmans, S. Li, T. Vail, A. K. Raap, R. S. Niedbala, and H. J. Tanke, Nat. Biotechnol. **19**, 273 (2001).
[5] S. Heer, K. Kömpe, H. Güdel, and M. Haase, Adv. Mater. (Weinheim, Ger.) **16**, 2102 (2004).
[6] G. Y. Chen, Y. G. Zhang, G. Somesfalean, Z. G. Zhang, Q. Sun, and F. P. Wang, Appl. Phys. Lett. **89**, 163105 (2006).
[7] K. Okamoto, I. Niki, A. Shvartser, Y. Narukawa, T. Mukai, and A. Scherer, Nat. Mater. **3**, 601 (2004).
[8] T. D. Neal, K. Okamoto, and A. Scherer, Opt. Express **13**, 5522 (2005).
[9] H. Mertens and A. Polman, Appl. Phys. Lett. **89**, 211107 (2006).
[10] S. Pillai, K. R. Catchpole, T. Trupke, G. Zhang, J. Zhao, and M. A. Green, Appl. Phys. Lett. **88**, 161102 (2006).
[11] Y. Zhang, K. Aslan, M. J. R. Previte, and C. D. Geddes, Appl. Phys. Lett. **90**, 173116 (2007).
[12] D. M. da Silva, L. R. P. Kassab, S. R. Lüthi, C. B. de Araújo, A. S. L. Gomes, and M. J. V. Bell, Appl. Phys. Lett. **90**, 081913 (2007).
[13] G. N. van den Hoven, E. Snoeks, A. Polman, C. van Dam, J. W. M. van Uffelen, and M. K. Smit, J. Appl. Phys. **79**, 1258 (1995).
[14] J. Gersten and A. Nitzan, J. Chem. Phys. **75**, 1139 (1981).
[15] M. Meier and A. Wakaun, Opt. Lett. **8**, 581 (1983).
[16] H. Sun, L. Zhang, J. Zhang, L. Wen, C. Yu, S. Dai, L. Hu, and Z. Jiang, Solid State Commun. **133**, 781 (2005).
[17] H. Guo, N. Dong, M. Yin, W. Zhang, L. Lou, and S. Xia, J. Phys. Chem. B **108**, 19205 (2004).
[18] G. A. Kumar, C. W. Chen, and R. E. Riman, Appl. Phys. Lett. **90**, 093123 (2007).